

Influence of rheological properties and microstructure of microemulsions on the kinetic release of bioactive compounds

Noelia Mori Cortés

Centro de Investigación y Desarrollo en Criotecnología de Alimentos

Sebastián Scioli Montoto

Laboratorio de Investigación y Desarrollo de Bioactivos (LIDEB)

María Esperanza Ruiz

Laboratorio de Investigación y Desarrollo de Bioactivos (LIDEB)

Alicia Califano

Centro de Investigación y Desarrollo en Criotecnología de Alimentos

Gabriel Lorenzo (✉ gabriel.lorenzo@ing.unlp.edu.ar)

Centro de Investigación y Desarrollo en Criotecnología de Alimentos

Research Article

Keywords: Microemulsions, viscoelasticity, bioactive compound release, relaxation time spectrum, carboxymethyl cellulose, vitamins

Posted Date: May 16th, 2022

DOI: <https://doi.org/10.21203/rs.3.rs-1631014/v1>

License:  This work is licensed under a Creative Commons Attribution 4.0 International License.

[Read Full License](#)

1 **Influence of rheological properties and microstructure of microemulsions on the**
2 **kinetic release of bioactive compounds**

3
4
5 Mori Cortés¹, Noelia; Scioli Montoto², Sebastián; Ruiz², María Esperanza; Califano¹,
6 Alicia N.; Lorenzo^{1,3*}, Gabriel

7
8
9
10 ¹ *Centro de Investigación y Desarrollo en Criotecología de Alimentos (CIDCA),*
11 *Facultad de Cs. Exactas, UNLP-CICPBA-CONICET. 47 y 116, La Plata (1900),*
12 *Argentina.*

13 ² *Laboratorio de Investigación y Desarrollo de Bioactivos (LIDeB, CONICET- Facultad*
14 *de Ciencias Exactas, UNLP) – Cátedra de Control de Calidad de Medicamentos*
15 *(Facultad de Ciencias Exactas, UNLP), 47 y 115, La Plata, Argentina.*

16 ³ *Departamento de Ingeniería Química, Facultad de Ingeniería, Universidad Nacional*
17 *de La Plata, Argentina.*

18 **corresponding author: TE/Fax: 54(221)4254853, 47 y 116 (1900) La Plata, Buenos.*
19 *Aires, ARGENTINA. Email: gabriel.lorenzo@ing.unlp.edu.ar*

20
21
22
23
24
25 **Acknowledgements**

26 The authors are grateful to BASF Argentina S.A., who provided the emulsifier for this
27 study and Laboratorios Bagó Argentina S.A. for provide the vitamins. The financial
28 support of the Consejo Nacional de Investigaciones Científicas y Técnicas (CONICET)
29 (PIP 0161 GI), Agencia Nacional de Promoción Científica y Tecnológica (PICT 2015-
30 0344 and PICT 2017-1129) and Universidad Nacional de La Plata (X873) is also
31 acknowledged.

32 In memory of Dr. Alicia Califano (1951–2019), Lead Scientist (CIDCA-CONICET,
33 Argentina) and a highly respected colleague who will be greatly missed.

35 **Abstract**

36 Microemulsions (ME) are one of the most effective ways to incorporate lipophilic active
37 compounds into water-based food matrices. Great stability, colloidal domain droplets,
38 and optical isotropy are some of the ME advantages. The present work analyzes the
39 influence of rheological behavior and microstructural characteristics of food
40 microemulsions on the release rate of lipophilic vitamins. A fluid ME was compared to
41 a ME with higher dispersed phase content and a bicontinuous structure (gel-ME).
42 Additionally, carboxymethyl cellulose (CMC) was added to fluid ME (3.5 and 10
43 g/100g), obtaining systems with different viscosity and microstructure. All ME were
44 characterized using FTIR, rheological analysis, and TEM microscopy. Those systems
45 with similar zero-shear viscosity showed significantly different viscoelastic behavior;
46 gel-ME behaved like a concentrated suspension of macromolecules but with the largest
47 plateau modulus. Microemulsions with CMC exhibited a viscoelastic solid type with G'
48 $> G''$. Mechanical spectra were satisfactorily fitted with Generalized Maxwell model
49 and the relaxation time spectra were determined. Kinetic release of vitamins E and D
50 was studied and modeled at 37 °C. Fluid and gel-ME reached higher percentages of
51 release in a very fast manner, while CMC systems showed a matrix-driven nature of the
52 release, in agreement with the relaxation time behavior determined from rheological
53 experiments.

54

55

56

57

58

59

60

61

62

63

64

65

66

67 **Keywords:** Microemulsions; viscoelasticity; bioactive compound release; relaxation
68 time spectrum; carboxymethyl cellulose; vitamins

69 **Author's Contribution**

70 **N.M.C.** participated in: Methodology, Investigation, Writing - Original Draft, Writing -
71 Review & Editing

72 **S.S.M.** contributed to: Methodology, Investigation, Writing - Review & Editing

73 **M.E.R.** worked mainly in: Conceptualization, Investigation, Writing - Review &
74 Editing, Supervision,

75 **A.C.** was a critical part in: Conceptualization, Project administration, Funding
76 acquisition

77 **G.L.** did a general contribution in: Conceptualization, Investigation, Writing - Review
78 & Editing, Project administration, Supervision, Funding acquisition.

79 **All authors read and approved the final manuscript.**

80

81 **Conflict of Interest**

82 The authors declare that they have no known competing financial interests or personal
83 relationships that could have appeared to influence the work reported in this paper.

84

85 **Funding**

86 - Consejo Nacional de Investigaciones Científicas y Técnicas (CONICET): *PIP 0161 GI*

87 - Agencia Nacional de Promoción Científica y Tecnológica: *PICT 2015-0344* and *PICT*

88 *2017-1129*

89 - Universidad Nacional de La Plata: *X873*

90 1. INTRODUCTION

91 In recent years, consumers' demand for functional foods has increased as a result
92 of the increased knowledge of functional ingredients and their impact on human health
93 and physiological functions [1, 2]. There are a wide variety of foods where lipophilic
94 active compounds (such as bioactive lipids, flavors, antimicrobials, antioxidants, and
95 nutraceuticals) must be incorporated into aqueous media, to make them suitable for oral
96 consumption [3, 4]. Particularly, vitamins are essential for human growth and
97 development, but most of them are not produced in the human body and need to be
98 supplied through foods or food supplements [1]. Adequate intake of vitamin D increases
99 the intestinal absorption of calcium and promotes normal bone formation and
100 mineralization [5, 6]. Vitamin E, on the other hand, provides health benefits to humans
101 such as the prevention of cardiovascular diseases and cancer [7, 8]. Furthermore,
102 vitamin E plays a fundamental role in the treatment of Alzheimer and other neurological
103 diseases [9].

104 Material and microstructures that can enable the controlled release of active
105 ingredients are increasingly used in both the foods and pharmaceutical industries [10].
106 Colloidal delivery systems such as microemulsions, nanoemulsions, and emulsions are
107 some of the most effective ways to encapsulate and incorporate lipophilic active
108 compounds into water-based matrices. These vehicle systems should be capable of
109 releasing the active compound after consumption at a particular site within the human
110 body, for example, bioactive compounds in the gastrointestinal tract and flavors in the
111 mouth [11]. Therefore, controlled release systems were developed to maintain the
112 desired concentration of the active compounds, exerting control on the release rate and
113 duration.

114 Microemulsions have been attracted the attention of the cosmetic and food
115 industries since they are optically isotropic, thermodynamically stable, and can improve
116 the bioavailability of bioactive compounds. Some studies indicate that the
117 bioavailability of bioactive compounds may be increased when delivered as an o/w
118 microemulsion because the interfacial layer of the nanodroplets can enhance
119 transmembrane passage across the digestive tract [12]. Additionally, most
120 microemulsions, mainly those with nonionic emulsifiers, presented great stability in a
121 wide range of pH, temperature, and ionic strength [13-15]. Furthermore, the
122 transparency of microemulsions allows the incorporation of lipophilic bioactive
123 compounds in wide variety of food matrices that must be transparent or have a slightly

124 cloudy appearance (i.e., flavored waters, herbal drinks, isotonic drinks, jellies, fruit
125 gummies, etc.).

126 From a structural point of view, microemulsions contain oil and water
127 microdomains separated by surfactant layers like lyotropic liquid crystals, which gives a
128 wide range of flow behaviors depending on the concentration of the components [16].
129 Thus, a fluid water-like microemulsion with tiny oil droplets could be obtained as well
130 as a gel-type bicontinuous structure altering layers of oil and water, depending on the
131 disperse phase content.

132 This great variety of structures and behavior makes microemulsions very
133 attractive systems for food applications as bioactive compounds delivery. However, the
134 interaction between components and the rheological behavior could probably affect the
135 way of bioactive compounds are released from a food matrix. Therefore, the hypothesis
136 of this work is that the kinetic release of bioactive compounds from the internal lipid
137 phases depends on both the viscosity of the continuous phase and the microemulsions
138 structure.

139 The objective of the present work was to analyze the influence of rheological
140 behavior and microstructural characteristics of food microemulsions on the release rate
141 of lipophilic vitamins.

142

143 **2. MATERIALS AND METHODS**

144 **2.1 Materials**

145 Macroglycerol hydroxystearate (Kolliphor RH40) was kindly donated by BASF
146 (Argentina S.A.). Commercial sunflower oil was purchased from Molinos Cañuelas
147 (SACIFIA, Argentina). Analytical grade ethanol > 99.5% was used as cosurfactant
148 (Soria, Argentina). Vitamin E acetate and vitamin D were provided by Laboratorios
149 Bagó (Argentina S.A.). Butylated hydroxytoluene (BHT) was used as antioxidant
150 (Sigma Aldrich, Argentina). Carboxymethyl cellulose (CMC) was employed as
151 thickener (Saporiti SACIFIA, Argentina). Sodium azide was used as antimicrobial agent
152 (Anedra, Argentina). Distilled water was added to all continuous phases and
153 microemulsions.

154

155 **2.2 Formation of continuous phases**

156 In order to formulate o/w microemulsions with thickener with a target viscosity, the
157 flow behavior of aqueous continuous phases with CMC was previously determined.

158 Dispersions with 3, 3.5, 4, and 5 g CMC/100 g water were evaluated. Samples were
159 prepared by slowly adding the hydrocolloid in a vessel with distilled water at 40°C and
160 with constant stirring. They were allowed to stand for 24 h before use.

161

162 **2.3 Formation of microemulsion**

163 Microemulsions were prepared following the procedure previously described with
164 slight modifications [14]. First, vitamins E and D (1:1) together with BHT (0.01 g/100 g
165 lipid phase) were dissolved in sunflower oil. Then, disperse phase was prepared by
166 mixing appropriate amounts of surfactant (Kolliphor RH40), sunflower oil and absolute
167 ethanol (cosurfactant). Microemulsions were prepared by slowly adding water over the
168 lipid phase with constant stirring. Depending on the water content, two microemulsions
169 were obtained: gel-ME (with a bicontinuous structure) and o/w-ME (fluid).
170 Additionally, two CMC concentrations were added to the o/w-ME, to obtain the low
171 CMC and high CMC microemulsions (Table 1).

172

173 **Table 1.** Composition of the studied microemulsions. Contents are given in g/100 g of
174 final microemulsion.

	o/w-ME	gel-ME	ME-low CMC	ME-high CMC
Water	80	40	76.5	70
Sunflower oil	0.67	3.34	0.67	0.67
Surfactant	18	54	18	18
Cosurfactant	0.67	2	0.67	0.67
Vit. E & D (1:1)	0.66	0.66	0.66	0.66
CMC	-	-	3.5	10

175

176

177 **2.4 Rheological measurements**

178 Rheological tests were carried out for the different formulations using a Haake
179 RS600 controlled stress rheometer (Haake, Germany). Parallel plates of 60 mm
180 diameter were used for the most viscous samples and double gap concentric cylinders
181 for the most fluid. All measurements were performed at least in duplicate and
182 maintaining a constant temperature of 37°C to simulate the thermal condition of the
183 release study. The data was processed using the IRIS Rheo-hub 2012 program to
184 perform the flow behavior and spectra calculations [17]. The standardized protocols

185 used were previously described by Mori Cortés et al. [14]. Briefly, steady state flow
186 measurements were applied to determine the viscosity dependence on the shear rate.
187 Additionally, stress sweeps were performed at a frequency of 1 Hz (6.28 rad/s) to
188 determine the linear viscoelastic range (LVR). Afterwards, within the LVR, frequency
189 sweeps were carried out to obtain the variation of the elastic (G') and viscous (G'')
190 moduli. Lastly, changes in the rheological behavior were monitored as a function of
191 time and over a temperature sweep (8°C-80°C), using a fixed stress within the LVR.

192

193 **2.5 Fourier-transform infrared spectroscopy (FTIR)**

194 Samples were analyzed using a Thermo Nicolet iS10 spectrometer (Thermo
195 Scientific, MA, USA) with an attenuated total reflectance (ATR) accessory. FTIR
196 spectra were recorded as a result of 32 consecutive scans and a resolution of 4 cm⁻¹.
197 Scanning was conducted from 4000 to 600 cm⁻¹. Before each determination a
198 background without sample was determined. At least four replicates of samples were
199 recorded. Spectrum analysis was performed using the software Omnic 9.0 (Thermo
200 Scientific, Madison, USA).

201

202 **2.6 Transmission electron microscopy (TEM)**

203 The microemulsions were observed with a transmission electron microscope (JEM
204 1200EX II, Jeol, USA) by using a negative staining method. A small aliquot of
205 microemulsion was deposited on a collodion coated grid and stained with one drop of
206 aqueous solution of phosphotungstic acid. The excess droplet was removed before TEM
207 observation.

208

209 **2.7 Release studies**

210 The release profiles of vitamins were determined using dissolution equipment (USP
211 Apparatus I, basket). Phosphate buffer (250 ml) at pH 6.8 was used as dissolution
212 medium. The temperature was set at 37°C and the dissolution medium was continuously
213 stirred at 50 rpm. The formulations were previously placed in rigid gelatin capsules
214 (two capsules per glass). At predetermined time intervals (0.5, 1, 2, 4, 6, 10 and 24
215 hours), 1 ml samples were taken and replaced by the same volume of fresh release
216 medium to maintain sink conditions at all times. The percentage of vitamins released
217 was determined in a Dionex Ultimate 3000 UHPLC (Thermo Scientific, Sunnyvale,
218 CA, USA) equipped with a dual gradient tertiary pump (DGP-3000) and a DAD-3000

219 diode array detector. A C18 column (Phenomenex, USA), packed with 5 μm particles
220 was utilized for chromatographic separation. Two wavelengths were selected for the
221 determination of vitamins in order to obtain greater sensitivity for the detection of each
222 one: 265 nm (vitamin D) and 284 nm (vitamin E).

223

224 **2.8 Statistical analysis**

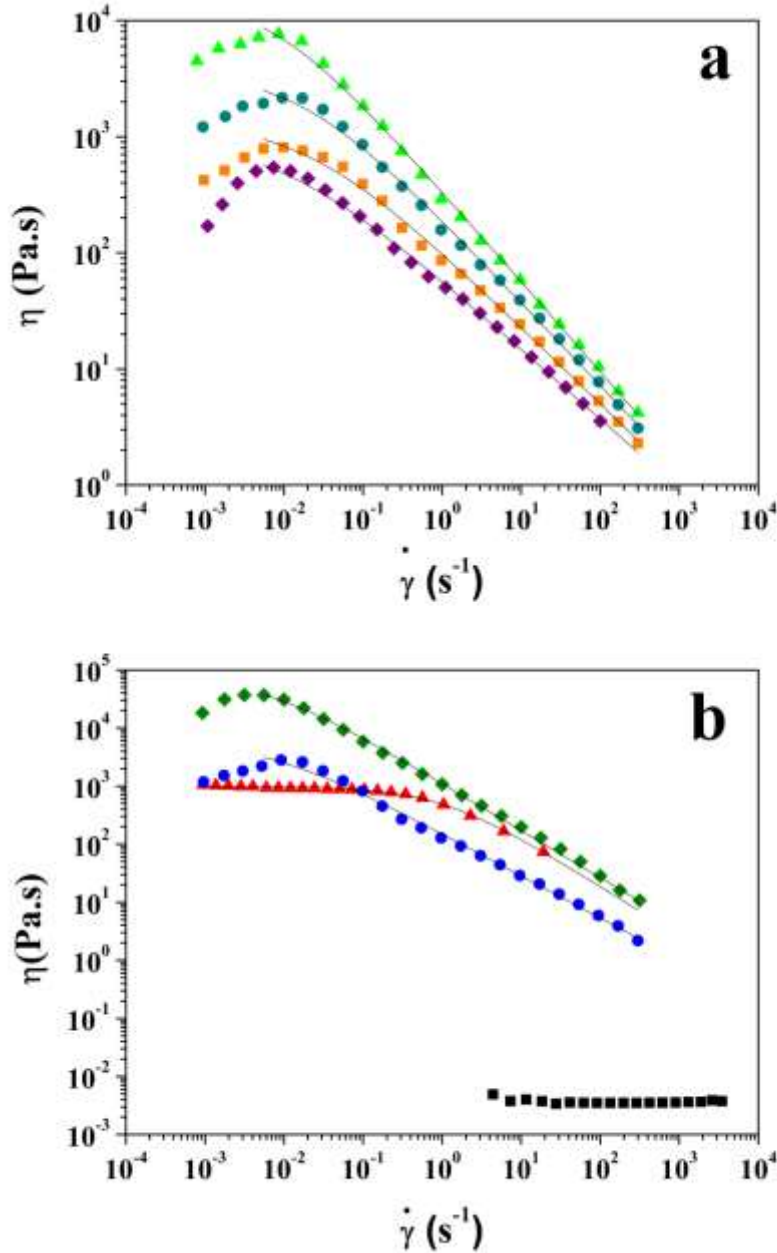
225 All statistical procedures were computed using the SYSTAT software (SYSTAT Inc.,
226 Evanston, IL, USA). Analyses of variance were conducted separately on the dependent
227 variables analyzed. Tukey's test was chosen for simultaneous pairwise comparisons.
228 Differences in means and F-tests were considered statistically significant when $P < 0.05$.

229

230 **3. RESULTS AND DISCUSSION**

231 **3.1 Flow behavior of the microemulsions**

232 Fig.1a shows the shear rate dependence of the viscosity for carboxymethyl cellulose
233 dispersions at different concentrations (3, 3.5, 4 and 5 g CMC/100 g), at a temperature
234 of 37°C. As it was previously reported, this rise in viscosity could be attributed to the
235 increase in the intermolecular interaction between CMC molecules [18]. All
236 suspensions exhibited a marked non-newtonian behavior, typical in concentrated
237 hydrocolloid dispersions. Although an overall shear-thinning behavior is observed for
238 all samples, it is noteworthy that at low shear rates, CMC suspensions showed a shear
239 thickening behavior. At large shear rates, macromolecule chains are disentangled and
240 aligned in the flow direction, which is the general consensus of the shear-thinning
241 behavior of biopolymeric suspensions. However, shear-thickening was not deeply
242 discussed and it is not fully elucidated. Benchabane and Bekkour [19] found the same
243 shear-thickening behavior in CMC suspensions and related with a stiffer inner structure
244 caused by the formation of entanglements between polymer coils and the increase in the
245 intermolecular interactions, as the shear rate rises.



246
 247 **Fig. 1** a) Flow curves of aqueous suspensions with different concentrations of
 248 carboxymethyl cellulose: (◆) 3, (■) 3.5, (●) 4 y (▲) 5 g CMC/100 g distilled water. b)
 249 Flow curves for microemulsions: (■) o/w-ME, (▲) gel-ME, (●) ME-low CMC and
 250 (◆) ME-high CMC according to Table 1 codes. Continuous line: Cross model

251

252 To interpret the shear thinning dependence, the Cross model was used [20]:

253

254
$$\eta = \frac{\eta_0}{(1+(\tau\dot{\gamma})^n)} \quad (1)$$

255

256 where η is the viscosity corresponding to a shear rate $\dot{\gamma}$; η_0 is the asymptotic value at
257 zero shear rate; τ is a transition time that represents the reciprocal of the shear rate
258 required to halve the viscosity, and n a measure of the pseudoplastic characteristics.

259 It was observed that by increasing the concentration of thickener from 3 to 5 g/100 g,
260 the value of η_0 increased from 9.7×10^2 to 1.6×10^4 Pa.s. This is because the CMC
261 generates a structure formed by a three-dimensional network of interconnected CMC
262 chains. Then, increasing their concentration increases the interactions between the
263 chains causing an increase in the strength of the network. As shown in Fig. 1b, the ME-
264 low CMC also exhibited a qualitatively similar behavior to the corresponding
265 continuous phase but with a marked increase in viscosity values. This suggests that the
266 oil droplets are trapped in the network formed by the polymer chains of CMC thus
267 reinforcing the structure.

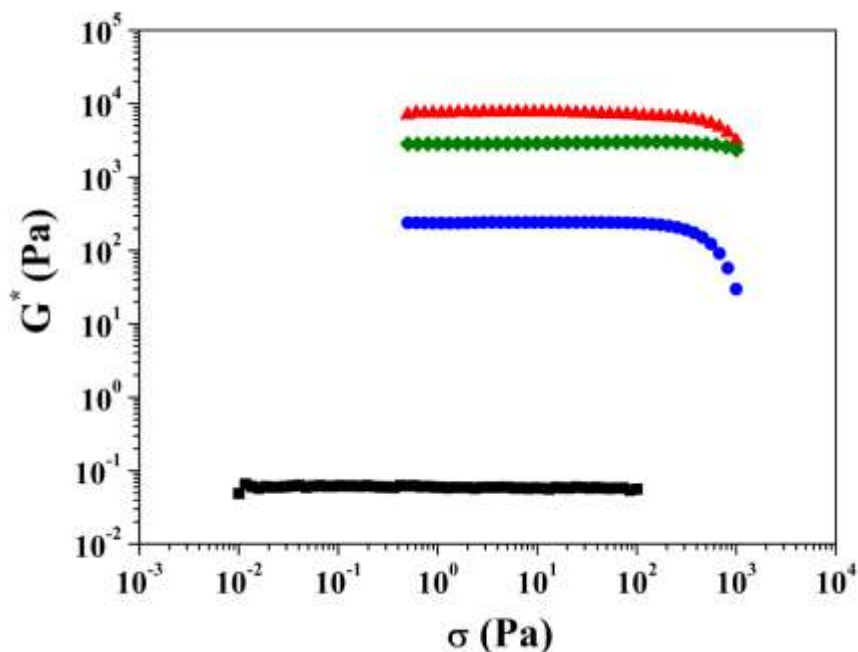
268 Fig. 1b shows that the gel-ME containing 60 g dispersed phase/100 g emulsion also
269 exhibited a marked pseudoplastic behavior. However, its behavior was qualitatively
270 different from ME-low CMC. Although both values of η_0 could be considered within
271 the same range (2.3×10^3 Pa.s and 9.9×10^2 Pa.s for the microemulsion with thickener and
272 gel, respectively), the values of τ were significantly different. The ME-low CMC had a
273 characteristic transition time of 30.2 s while for the gel-ME it was only 1.02 s. This
274 value corresponds to the inverse of the shear rate that is necessary for the structure of
275 the material to begin to flow. Therefore, gel-ME presented a more stable structure and a
276 greater range of deformation rates without modifying its viscosity. On the other hand,
277 microemulsion containing 10 g CMC/100 g (ME-high CMC) exhibited pseudoplastic
278 behavior with a value of $\eta_0 = 7.6 \times 10^4$ Pa.s. This microemulsion presented a transition
279 time ($\tau = 58.7$ s) longer than ME-low CMC. At rest, the microemulsion with higher
280 thickener content has a stronger structure given by the greater number of interactions
281 between the CMC polymer chains. However, by increasing the shear stress these
282 interactions are easily broken causing weakening of the structure.

283 The decrease in the dispersed phase content at 20 g disperse phase/100 g emulsion
284 generated changes in the flow characteristics of the microemulsion. The o/w-ME
285 exhibited a Newtonian behavior. This behavior is characteristic of microemulsions
286 where oil drops are freely dispersed in a large volume of continuous phase.

287

288 **3.2 Viscoelastic behavior of microemulsions**

289 Stress sweeps of the different microemulsions were carried out to determine their
 290 linear viscoelastic range. Fig. 2 shows the complex modulus ($G^* = ((G')^2 + (G'')^2)^{1/2}$) as
 291 a function of the stress amplitude. The fluid o/w-ME was invariant throughout the entire
 292 range of measured stresses. While the gelled microemulsions either by the addition of
 293 thickener or by the increase of disperse phase showed a decrease of G^* to
 294 approximately 300 Pa.



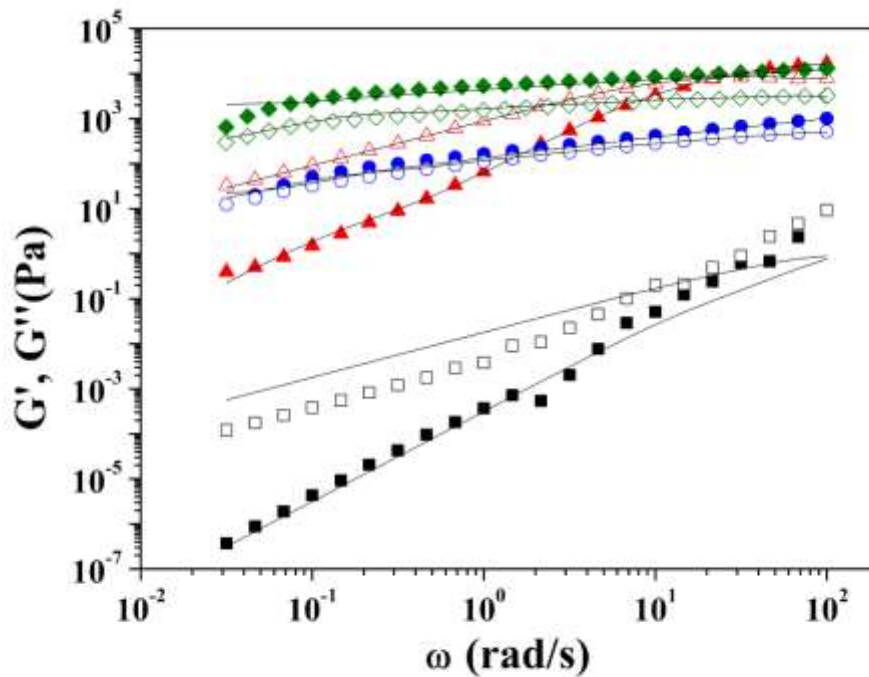
295
 296 **Fig. 2** Stress sweeps for microemulsions: (■) o/w-ME, (▲) gel-ME, (●) ME-low
 297 CMC and (◆) ME-high CMC according to Table 1

298
 299 Fig. 3 shows the elastic modulus (G') and the viscous modulus (G'') as a function of
 300 the oscillatory frequency (ω) at 37°C. It can be seen that although the ME-low CMC
 301 and the gel-ME had similar zero-shear viscosities, they exhibited a markedly different
 302 viscoelastic behavior. The gel-ME showed characteristics of a concentrated solution of
 303 macromolecules with $G'' > G'$ and a crossover of both moduli at $\omega \sim 25$ rad/s. On the
 304 contrary, both o/w microemulsions containing thickener exhibited a viscoelastic solid
 305 type behavior with $G' > G''$ throughout the studied frequency range and with a low
 306 dependence of both moduli with the frequency. Although the ME-low CMC exhibited a
 307 weak gel-like behavior, its mechanical spectrum was below the gel-ME spectrum. As
 308 the thickener content increased, there was an increase in the elastic characteristics of the
 309 system. Thus, the ME-high CMC showed a significant increase in both moduli,

310 exceeding the mechanical spectra of the gel-ME. Larger differences between G' and G''
 311 and a smaller variation with oscillation frequency were observed, which is a typical
 312 behavior of a more elastic matrix. On the other hand, the o/w-ME exhibited a markedly
 313 viscous behavior, typical of a Newtonian fluid. Very low values of G' and G'' and a
 314 marked linear dependence of these parameters were observed with frequency
 315 throughout the studied range ($G' \propto \omega^2$ and $G'' \propto \omega$).

316 The results obtained were adjusted satisfactorily using the generalized Maxwell
 317 model, where the values of G' and G'' at each frequency are given by the sum of N
 318 contributions from N Maxwell elements in parallel, defined by the elastic response of a
 319 spring (G_i) and the relaxation time λ_i [21].

320



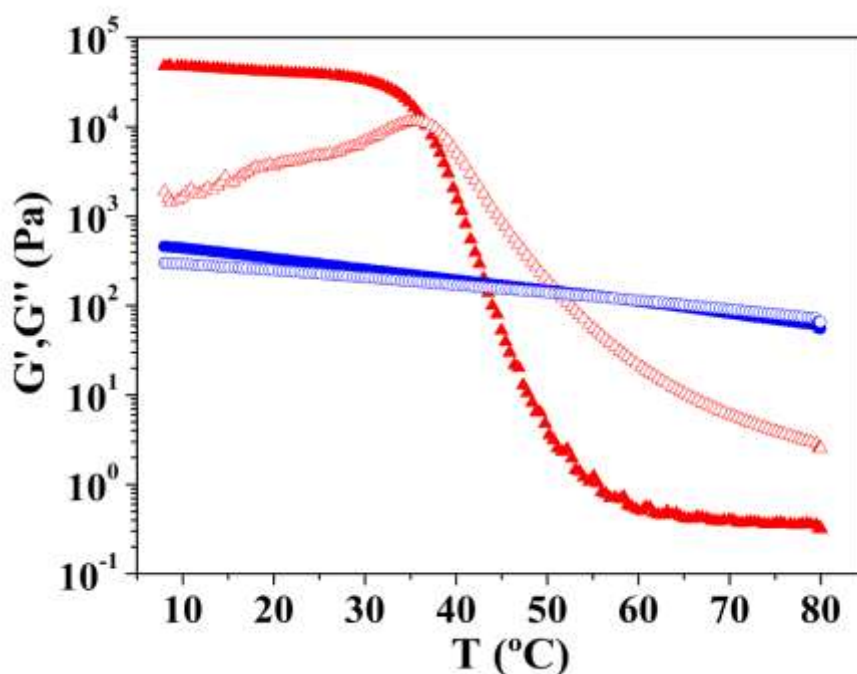
321
 322 **Fig. 3** Frequency sweeps for microemulsions: (■,□) o/w-ME, (▲,△) gel-ME, (●○)
 323 ME-low CMC and (◆,◇) ME-high CMC, according to Table 1. Full symbols: G' ;
 324 empty symbols: G'' . Continuous lines: Maxwell model

325

326 3.3 Thermo-rheological analysis

327 Fig. 4 shows G' and G'' vs temperature for the gel-ME and ME-low CMC. The
 328 microemulsions showed markedly different behaviors with temperature. At low
 329 temperature, the gel-ME constituted a stronger gel than the ME-low CMC. However,

330 when the temperature increased, an abrupt fall of both moduli and a crossover at 36.5°C
 331 were observed. This behavior is associated with the thermal properties of the emulsifier
 332 that were previously reported in other works, where an abrupt fall in the complex
 333 viscosity η^* of the Kolliphor RH40 was observed at a similar temperature, related to its
 334 complete fusion [14]. Conversely, the ME-low CMC showed a slight variation of the
 335 moduli with the temperature and a crossover of G' and G'' at around 60°C. This
 336 behavior is similar to that previously reported in CMC suspensions, which shows that
 337 the rheology of the hydrocolloid governs the mechanical properties of microemulsions
 338 [22]. Both the o/w microemulsion with thickener and gelled completely recovered their
 339 structure after the cooling process (supplementary material S1).



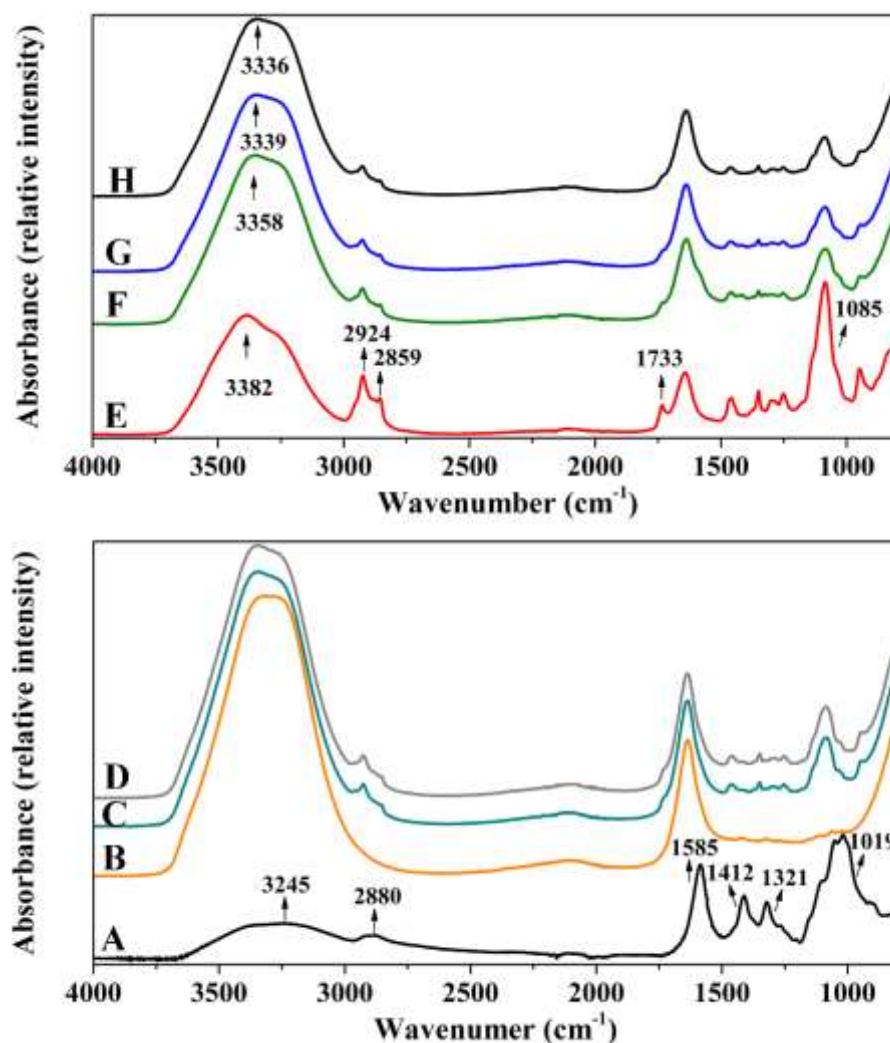
340
 341 **Fig. 4** Thermo-rheological analysis: ($\blacktriangle, \triangle$) gel-ME and (\bullet, \circ) ME-low CMC
 342 according to Table 1. Full symbols: G' ; empty symbols: G''

343

344 3.4. FTIR Analysis

345 To evaluate the interactions involved in the formation of the microemulsion, ATR-
 346 FTIR spectra was determined (Fig. 5) on CMC (A), hydrogels of CMC (B),
 347 CMC+Kolliphor RH40 (C), and CMC+Kolliphor RH40+ethanol (D), o/w-ME (E), ME-
 348 low CMC (F), ME-high CMC (G) and gel-ME (H). The FTIR spectrum of CMC (A)
 349 showed a broad band at 3245 cm^{-1} due to the $-\text{COO}$ stretching, which overlaps with the
 350 $-\text{OH}$ stretching region at $3400\text{--}3300\text{ cm}^{-1}$ [23]. The band at 2880 cm^{-1} arises from the

351 C–H stretching. The peak at 1585 cm^{-1} was attributed to asymmetric stretching of –
352 COO group. The bands around 1412 and 1321 cm^{-1} were assigned to $-\text{CH}_2$ scissoring
353 and C–OH bending vibration, respectively [24]. The band at 1019 cm^{-1} was associated
354 with $\text{CH}_2\text{–O–CH}_2$ stretching. FTIR of the hydrogels (B, C, and D) and microemulsions
355 (E, F, G, and H) presented a peak at 1635 cm^{-1} , assigned to the scissoring vibration of
356 water and a broad band around $3650\text{--}3000\text{ cm}^{-1}$ corresponding to the asymmetric
357 stretching and hydrogen bonds of the $-\text{OH}$ group. The band in the $3650\text{--}3000\text{ cm}^{-1}$
358 region can be divided into a lower frequencies band ($3300\text{--}3000\text{ cm}^{-1}$) corresponding to
359 strong hydrogen bonds arranged in a tetrahedral structure, and a higher frequencies band
360 ($3650\text{--}3300\text{ cm}^{-1}$), related to weak hydrogen bonds (non-tetrahedral ordering) of water
361 molecules. Compared to pure water, the spectra of microemulsions showed a decrease
362 in the relative area of the band around 3250 cm^{-1} , which is a measure of the fraction of
363 water molecules that vibrates within a tetrahedral structure [25]. Additionally, a shift of
364 the vibration frequency was observed from 3313 cm^{-1} in pure water to 3382 cm^{-1} in gel-
365 ME that could be attributed to hydrogen bond weakening. Similar results were reported
366 by Moayedzadeh, Gunasekaran, and Madadlou [26] when studying gelled emulsions
367 with gellan gum. On the other hand, by subtracting the spectral contribution of water to
368 the spectrum of the hydrogels and the microemulsions, some of the characteristic peaks
369 of CMC and surfactant could be observed (supplementary material S2). All the
370 microemulsions presented a band with two peaks at approximately 2924 and 2859 cm^{-1}
371 that were attributed to asymmetric and symmetric $-\text{CH}_2$ stretching vibrations,
372 respectively. While the peak at 1733 cm^{-1} was assigned to the C=O stretching [27].
373 Furthermore, the microemulsion showed an intense band at 1085 cm^{-1} due to C–O–C
374 stretching. These peaks were assigned to the surfactant since they were not found in the
375 CMC or in CMC hydrogel.



376
 377 **Fig. 5** ATR-FTIR spectra of CMC (A), hydrogels of CMC (B), CMC+Kolliphor RH40
 378 (C), CMC+Kolliphor RH40+ ethanol (D), o/w-ME (E), ME-low CMC (F), ME-high
 379 CMC (G) and gel-ME (H), according to Table 1

380

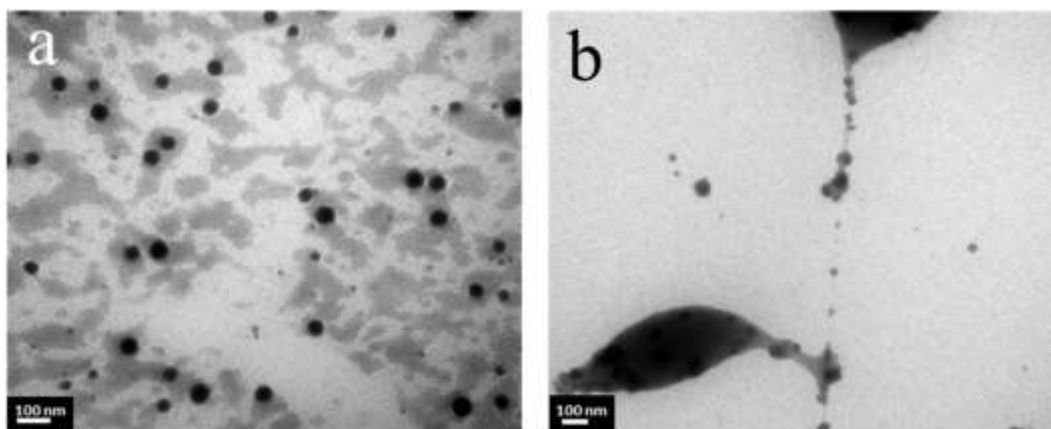
381

382 3.5 Transmission electron microscopy

383 In Fig. 6 the images obtained by TEM can be observed. The o/w-ME presented
 384 small spherical droplets homogeneously dispersed without presence of aggregates. For
 385 TEM observations it was necessary to eliminate the thickener from the continuous
 386 phase since it interfered with the observation of the drops. In the gel-ME, filamentous
 387 aggregates that interconnect irregular clusters of droplets were observed. Guo, Zhang,
 388 Wang, Liu, and Gu [28] observed a similar transition in microstructural characteristics
 389 when increasing the disperse phase content. The extended network of interconnected

390 particles and emulsifier micelles could be the responsible for the significant increase in
391 viscosity and elastic characteristics reported earlier.

392



393

394 **Fig. 6** Microscopic images obtained by TEM for: (a) o/w-ME and (b) gel-ME according
395 to Table 1

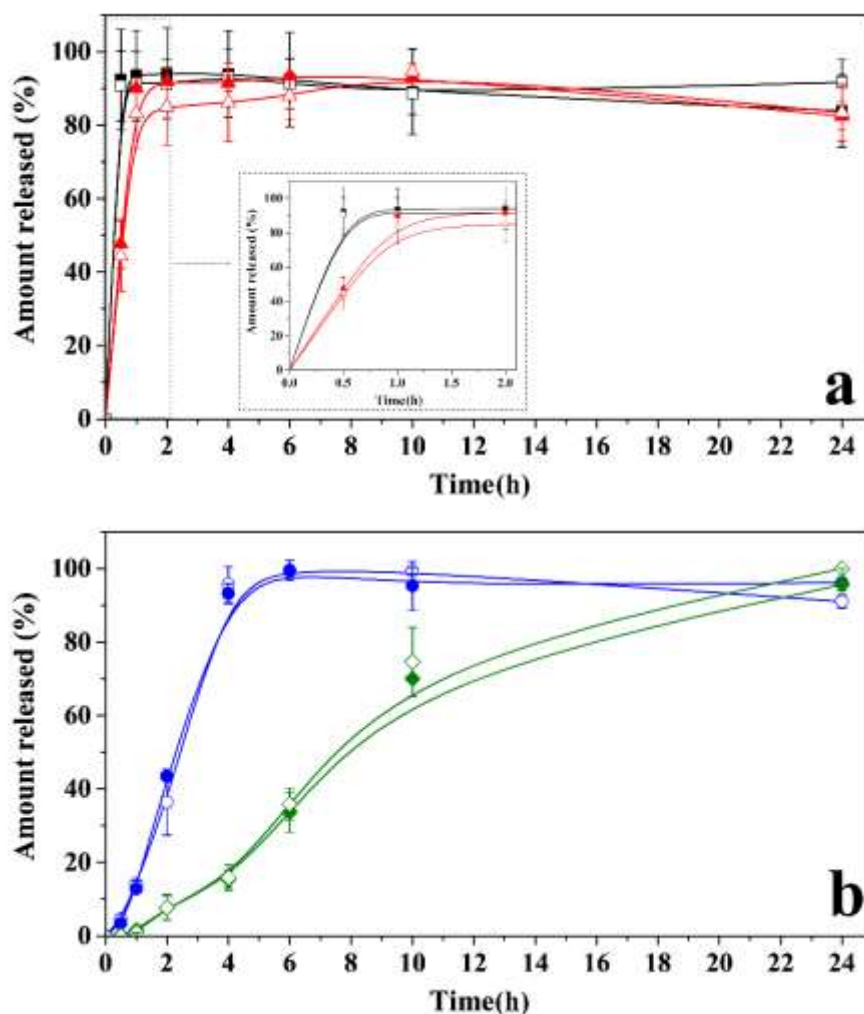
396

397 **3.6 Release studies**

398 Before the release assays, each component of the sample was analyzed separately
399 by HPLC (surfactant, sunflower oil, BHT and CMC) to detect possible interference
400 (peak overlap) with the bioactives. The BHT showed a chromatographic peak at
401 retention times markedly different from the retention times corresponding to the
402 vitamins, so no interference was observed. On the other hand, surfactant, sunflower oil
403 and CMC could not be detected under the chromatographic conditions tested. This
404 demonstrates that the usual concentrations of alpha-tocopherol from sunflower oil have
405 no detectable absorption peaks, which can overlap and interfere with the detection of
406 vitamin E incorporated in the microemulsion.

407 Fig. 7 shows the release profiles of vitamins E and D as a function of time for the
408 studied formulations. Vitamins E and D showed similar release rate regardless of the
409 type of structure or viscosity of the microemulsion. Initially there was a marked
410 difference in the release profile of the fluid o/w-ME and gel-ME (bicontinuous
411 structure). After 30 minutes, the o/w-ME presented more than 90% of the vitamins
412 release while the gel-ME showed a release ~45% for all bioactive components (Fig. 7a).
413 However, after 1 hour of testing, no significant differences were observed between the
414 release profiles of both microemulsions. Feng, Wang, Zhang, Wang, and Liu [29] found
415 similar results of the amount released when studying the rate of release of vitamin E in

416 o/w microemulsions produced with a non-ionic emulsifier. The release rate of bioactives
 417 in o/w-ME was mainly affected by the gradient concentration. In these systems, the oil
 418 droplets containing the bioactives were dispersed in an aqueous medium with low
 419 viscosity whereby they could easily diffuse into the release medium. On the other hand,
 420 the gel-ME having a higher viscosity had a lower diffusion coefficient and consequently
 421 a lower release rate.



422
 423 **Fig. 7** Vitamins release percentage as a function of time for (a) o/w-ME (■,□),gel-ME
 424 (▲,△), (b) ME-low CMC (●○) and ME-high CMC (◆,◇), according to Table 1. Full
 425 symbols: vitamin D; empty symbols: vitamin E. The inset in (a) corresponded to a zoom
 426 in the first 2h of release

427

428 However, the present study showed that changes in viscosity were not the only
 429 variable that affected the kinetic release. Gel-ME (bicontinuous structure) and ME-low
 430 CMC were formulated with similar zero-shear viscosity at the test temperature ($\eta \sim$

431 $1 \times 10^3 \text{Pa}\cdot\text{s}$ for $\dot{\gamma} < 0.01 \text{ s}^{-1}$) and exhibited notable differences in their release profiles (Fig.
432 7b). This suggests that the formation of a bicontinuous structure, where there are
433 bilayers of surfactant molecules containing alternate layers of oil and water, could allow
434 a greater availability of bioactives to diffuse into the release medium. Conversely, in the
435 microemulsion with CMC, the oil droplets with bioactives are immobilized in a network
436 formed by the entanglements of the polymeric chains of the thickener. The addition of
437 CMC to the fluid o/w-ME led to a marked decrease in the release rate of the bioactives.
438 The ME-low CMC presented a release below 5% after 30 minutes and only after 4
439 hours could release more than 90% of vitamins. The rate reduction effect was enhanced
440 by increasing the hydrocolloid concentration up to 10 g CMC/100 g since after 30
441 minutes the release percentage was less than 0.3% and only about 75% of vitamins were
442 released after 10 hours of testing. Feng, Xiong, Wang, and Yang [29] have reported that
443 the addition of a gelling agent to the continuous phase of a w/o microemulsion
444 decreased the release rate of the bioactives contained in the dispersed phase.

445

446 **3.7 Mathematical model of release profiles**

447 According to the shape of the release profiles obtained with all the assayed systems, it
448 was decided to adjust the simplest expression of the Korsmeyer-Peppas model, also
449 called *Power Law* [30]. This simple model has the advantage of a high degree of
450 flexibility: it can be adjusted to different release mechanisms according to the value of
451 the exponent (Equation 2).

$$452 \quad f_t = \frac{M_t}{M_\infty} = k \cdot t^n \quad (2)$$

453 It is a semi-empirical model initially developed to describe the release of a drug from a
454 polymeric matrix, such as a hydrogel [31]. In the equation, M_t and M_∞ are the
455 cumulative amounts of the compound released at time t and infinite time, respectively;
456 k contains structural and geometric information about the matrix or device, and n is
457 indicative of the drug release mechanism. To determine the exponent n , it is
458 recommended to use the first portion of the release curves, approximately until
459 $M_t/M_\infty \leq 0.60$ [32]. Thus, only the slow release systems were modelled, since the fluid
460 o/w-ME and the gel-ME reached that percentage of release in a very fast manner (less
461 than 1 h in both cases).

462 Model fitting was made first for each system (ME-low CMC and ME-high CMC) and
 463 for each vitamin (D and E) separately. However, it was observed that there were no
 464 significant differences between the estimates of the parameters by drug, and therefore it
 465 was decided to group the data into two unique models (ME-low CMC and ME-high
 466 CMC). The fact that a single model fits both vitamins means that the release profiles do
 467 not depend on the encapsulated compound, but only on the matrix. At the same time,
 468 grouping the data allows the estimation of the parameters with greater precision.
 469 The results of the modelling analysis are shown in Table 2, along with some goodness
 470 of fit measures.

471

472 **Table 2.** Modelling analysis of the vitamins' release profiles

ME-low CMC (N=20)*			
Parameter	Estimate	Std. Error	p-value
k	15.0604	1.0172	<0.0001
n	1.3280	0.0521	<0.0001
<i>R: 0.9913; Adj-R: 0.9908; Error MS: 11.93; Regression p-value <0.0001</i>			
ME-high CMC (N=28)*			
Parameter	Estimate	Std. Error	p-value
k	2.1419	0.3037	<0.0001
n	1.5300	0.0649	<0.0001
<i>R: 0.9859; Adj-R: 0.9853; Error MS: 9.38; Regression p-value <0.0001</i>			

* For the fitting, time points until a minimum of 60% of release were used
 (i.e., until 4 h for ME-low CMC, and 10 h for ME-high CMC)

473

474

475 As it can be seen in Table 2, both models exhibit a value of $n > 1$, corresponding to the
 476 so-called Super Case II transport, and extreme form of transport representing purely
 477 relaxational behavior [33].

478 This matrix-driven nature of the release is in accordance to the fact that both vitamins
 479 fitted into the same model.

480 It is worth mentioning that the Korsmeyer-Peppas model that considers a lag time (t_{lag}),
 481 fitted slightly better in all cases, with estimated t_{lag} between 10 and 15 min (data not
 482 shown). However, we decided to use the model without t_{lag} (Eq. 2) because the observed

483 lag time corresponded to the delay imposed by the rigid gelatin capsule used during the
484 release test, so it was not justified to incorporate one more parameter to the model.
485 Resuming the analysis, the addition of CMC to the o/w-ME generated a polymeric
486 matrix where the oil droplets with bioactives were homogeneously dispersed. When the
487 system contacted the dissolution medium, an interface buffer/polymer matrix was
488 generated, with the corresponding concentration gradient. This could induce a buffer
489 flow into the microemulsion, causing a matrix swelling and, therefore, an increase in the
490 dimensions of the system. Consequently, this gain in the aqueous medium could
491 increase the mobility of the polymer chains, allowing the droplets of the microemulsion
492 to come into contact with the surrounding environment and diffuse out of the expanded
493 matrix. In these types of polymeric matrices, with strong interaction with the release
494 medium, its expansion will depend on the physicochemical properties, such as viscosity
495 [34]. As the concentration of CMC increases, a more closed structure was generated.
496 Thus, the steric hindrance of the polymer chains within the crosslinked networks
497 increased and consequently, the tortuosity of the diffusion path to the release
498 medium. Based on the model results, the release rate of the bioactives from
499 microemulsions depended not only on the dissolution rate of the bioactive but mainly on
500 the entanglements between hydrocolloids molecules that affect the relaxation of the
501 microstructure. Chain entanglement is probably best regarded as a special type of
502 intermolecular interaction, affecting mainly the large-scale motions of the chains, and
503 through them, the long time end of the viscoelastic relaxation time spectrum [35]. The
504 mechanical properties of microemulsions obtained with rheological analysis could be
505 useful to explain the differences observed in the release rate. Using the Maxwell
506 elements previously determined (G_i , λ_i), the plateau modulus and the characteristic
507 relaxation time were calculated as it was expressed by several authors [36, 37]:

508

$$509 \quad G_0^N = \sum_{i=1}^N G_i \quad (3)$$

510

$$511 \quad \lambda_{char} = \frac{\sum_{i=1}^N G_i \lambda_i^2}{\sum_{i=1}^N G_i \lambda_i} \quad (4)$$

512

513 The plateau modulus showed an increase in the elastic properties of the matrix in the
514 order: fluid o/w-ME < ME-low CMC < ME-high CMC < gel-ME with values of 1.89 Pa,
515 1.58×10^3 Pa, 1.49×10^4 Pa, 2.70×10^4 Pa, respectively. In the quiescent state, gel-ME

516 exhibited higher elastic behavior than those containing large amount of thickener in the
517 continuous phase. Conversely, λ_{char} showed a different behavior, increasing in the order:
518 fluid o/w-ME < gel-ME < ME-low CMC < ME-high CMC, with values of 1.75×10^{-2} s,
519 2.55×10^{-1} s, 4.74×10^2 s, 1.11×10^3 s, respectively. This behavior is in agreement with the
520 release profile obtained. The rise in the longest relaxation time of the matrices with the
521 increase in CMC concentration could be related to the delay in the large-scale chain
522 motions associated with the loosening of the interconnected structure and the
523 consequent droplet release.

524 Several authors have investigated the processes of hydrogel swelling and polymer
525 relaxation concerning controlled-release drug delivery systems [38, 39]. They relate it to
526 both the penetrant transport mechanism and the concurrent drug release mechanism
527 assuming the relaxation time for the hydrogels as a characteristic time for diffusion.
528 Particularly, with physical gels like those containing CMC, not only the relaxation
529 behavior of the hydrated macromolecules influences on bioactive release rate and water
530 penetration but also the structure of the gel layer [40]. Hence, in the quiescent state, the
531 higher zero-shear viscosity concurred with the lower kinetic release and with the longer
532 relaxation times.

533 On the other hand, the significantly different microstructure of gel-ME showed a rapid
534 drug release that could be related to the almost instantaneous dilution of the lipophilic
535 phase in the aqueous medium without the additional resistance of the polymeric matrix
536 swelling.

537

538 **4. Conclusion**

539 The present study showed that different strategies to obtain gel microemulsion could be
540 useful in controlling the release rate of bioactive compounds from the lipophilic phase,
541 which is in agreement with the hypothesis stated in this work. Increasing the dispersed
542 phase content to a fluid o/w-ME generated a gel-ME (with bicontinuous structure), with
543 a similar zero-shear viscosity (η_0) to those obtained using CMC in the continuous phase.
544 However, a markedly different viscoelastic behavior was observed. The thickener
545 addition generated systems with weak gels characteristics ($G' > G''$) and a slight
546 variation of both moduli with temperature. This greater structure stability was reflected
547 in the decrease in the release rate of vitamins. In other words, CMC not only controls
548 the mechanical properties of the microemulsion but also, the release rate of the bioactive
549 compound, by controlling the relaxation time of the polymeric entanglements.

550 Conversely, microemulsions with a bicontinuous structure resulted in a highly
551 viscoelastic matrix, which is useful to incorporate in different food systems without
552 significantly altering the bioavailability of bioactive compounds of a fluid
553 microemulsion. Therefore, by changing the viscoelasticity of the microemulsion, it is
554 possible to control the kinetic release of lipophilic components with different chemical
555 structure and behavior incorporated in gelled microemulsions.

556

557 **References**

- 558 [1] K.P. Velikov, E. Pelan, *Soft Matter*.(2008) <https://doi.org/10.1039/B804863K>
- 559 [2] M. Zeinalzadegan, M. Nejadmansouri, M.T. Golmakani, G.R. Mesbahi, D.J.
560 McClements, S.M. Hosseini, *Food Biophys.* (2021) [https://doi.org/10.1007/s11483-020-](https://doi.org/10.1007/s11483-020-09662-8)
561 [09662-8](https://doi.org/10.1007/s11483-020-09662-8)
- 562 [3] P.S. Given Jr., *Curr Op Colloid Interface Sci.* (2009)
563 <https://doi.org/10.1016/j.cocis.2008.01.007>
- 564 [4] L. Stounbjerg, C. Vestergaard, B. Andreasen, R. Ipsen, R, *Food Rev Int.* (2018)
565 <https://doi.org/10.1080/87559129.2017.1373286>
- 566 [5] A. Cranney, H.A. Weiler, S. O'Donnell, L. Puil, *Am J Clin Nutr.* (2008)
567 <https://doi.org/10.1093/ajcn/88.2.513S>
- 568 [6] N. Gueli, W. Verrusio, A. Linguanti, F. Di Maio, A. Martinez, B. Marigliano, M.
569 Cacciafesta, *Arch Gerontol Geriatr.* (2012)
570 <https://doi.org/10.1016/j.archger.2011.03.001>
- 571 [7] F. Galli, A. Azzi, M Birringer, J.M. Cook-Mills, M. Eggersdorfer, J. Frank, G.
572 Cruciani, S. Lorkowski, N.K. Özer, *Free Radic Biol Med.* (2017)
573 <https://doi.org/10.1016/j.freeradbiomed.2016.09.017>
- 574 [8] J.M. Zingg, A. Azzi, *Curr Med Chem.* (2004)
575 <https://doi.org/10.2174/0929867043365332>
- 576 [9] M. Grundman, *Am J Clin Nutr.* (2000). <https://doi.org/10.1093/ajcn/71.2.630s>
- 577 [10] F. Smaniotto, I. Zafeiri, V. Prosapio, F. Spyropoulos, *Food Struct.* (2021)
578 <https://doi.org/10.1016/j.foostr.2021.100179>
- 579 [11] K. Ziani, Y. Fang, D.J. McClements, *Food Chem.* (2012).
580 <https://doi.org/10.1016/j.foodchem.2012.03.027>
- 581 [12] M. Bergonzi, R. Hamdouch, F. Mazzacuva, B. Isacchi, A. Bilia, *LWT.* (2014)
582 <https://doi.org/10.1016/j.lwt.2014.06.009>

- 583 [13] M. Hou, T. Liu, B. Zhang, B. Chen, Q. Li, X. Liu, C. Lu, Z. Wang, L. Dang, Food
584 Chem. (2018) <https://doi.org/10.1016/j.foodchem.2018.02.100>
- 585 [14] N. Mori Cortés, A.N. Califano, G. Lorenzo, Food Res Int. (2019)
586 <https://doi.org/10.1016/j.foodres.2019.01.067>
- 587 [15] F. Valoppi, R. Frisina, S. Calligaris, Food Biophys. (2017)
588 <https://doi.org/10.1007/s11483-017-9480-9>
- 589 [16] D. Langevin, Mol Cryst Liq Cryst. (1986)
590 <https://doi.org/10.1080/00268948608071764>
- 591 [17] H.H. Winter, M. Mours, Rheol Acta. (2006) [https://doi.org/10.1007/s00397-005-](https://doi.org/10.1007/s00397-005-0041-7)
592 [0041-7](https://doi.org/10.1007/s00397-005-0041-7)
- 593 [18] K. Bekkour, D. Sun-Waterhouse, S.S. Wadhwa, Food Res Int. (2014)
594 <https://doi.org/10.1016/j.foodres.2014.09.016>
- 595 [19] A. Benchabane, K. Bekkour, Colloid Polym Sci. (2008)
596 <https://doi.org/10.1007/s00396-008-1882-2>
- 597 [20] J.F. Steffe, Rheological methods in food process engineering (Freeman Press,
598 1996).
- 599 [21] G. Lorenzo, N.E. Zaritzky, A.N. Califano, Carbohydr Polym. (2015)
600 <https://doi.org/10.1016/j.carbpol.2014.10.040>
- 601 [22] R.L. Feddersen, S.N. Thorp, in Industrial Gums ed. By R.L. Whistler, J.N.
602 BeMiller (Academic Press, 1993), p. 537
- 603 [23] A. Mirzaei-Mohkam, F. Garavand, D. Dehnad, J. Keramat, A. Nasirpour, Prog Org
604 Coat. (2020) <https://doi.org/10.1016/j.porgcoat.2019.105383>
- 605 [24] D. Biswal, R. Singh, Carbohydr Polym. (2004)
606 <https://doi.org/10.1016/j.carbpol.2004.04.020>
- 607 [25] T. Pintado, C. Ruiz-Capillas, F. Jiménez-Colmenero, P. Carmona, A.M. Herrero,
608 Food Chem. (2015) <https://doi.org/10.1016/j.foodchem.2015.04.024>
- 609 [26] S. Moayedzadeh, S. Gunasekaran, A. Madadlou, Food Hydrocoll. (2018)
610 <https://doi.org/10.1016/j.foodhyd.2018.03.042>
- 611 [27] G.M. El Maghraby, S.F. Ghanem, Int J Pharm Pharm Sci. 8, 127 (2016)
- 612 [28] J. Guo, L. Zhang, Y. Wang, T. Liu, X. Gu, Colloids Surf A Physicochem Eng Asp.
613 (2019) <https://doi.org/10.1016/j.colsurfa.2019.01.041>
- 614 [29] G. Feng, Y. Xiong, H. Wang, Y. Yang, Eur J Pharm Biopharm. (2009)
615 <https://doi.org/10.1016/j.ejpb.2008.08.014>

616 [30] P. Costa, J.M. Sousa Lobo, Eur J Pharm Sci. (2001) <https://doi.org/10.1016/S0928->
617 [0987\(01\)00095-1](https://doi.org/10.1016/S0928-0987(01)00095-1)

618 [31] R.W. Korsmeyer, R. Gurny, E. Doelker, P. Buri, N.A. Peppas, Int J Pharm. (1983)
619 [https://doi.org/10.1016/0378-5173\(83\)90064-9](https://doi.org/10.1016/0378-5173(83)90064-9)

620 [32] P.L. Ritger, N.A. Peppas, J Control Release. (1987) <https://doi.org/10.1016/0168->
621 [3659\(87\)90034-4](https://doi.org/10.1016/0168-3659(87)90034-4)

622 [33] H. Kim, R. Fassihi, J Pharm Sci. (1997). <https://doi.org/10.1021/js960307p>

623 [34] J. Siepmann, N.A. Peppas, Adv Drug Deliv Rev. (2012)
624 <https://doi.org/10.1016/j.addr.2012.09.028>

625 [35] W.W. Graessley, The entanglement concept in polymer rheology (Springer, 1974).

626 [36] M. Grassi, R. Lapasin, T. Coviello, P. Matricardi, C. Di Meo, F. Alhaique,
627 Carbohydr Polym. (2009) <https://doi.org/10.1016/j.carbpol.2009.04.025>

628 [37] M. Mours, H.H. Winter, IRIS rheo-hub handbook. Part D: Analysis of experiments.
629 (Iris Development LLC, 2011)

630 [38] V. Michailova, S. Titeva, R. Kotsilkova, J Drug Deliv Sci Technol. (2005)
631 [https://doi.org/10.1016/S1773-2247\(05\)50086-8](https://doi.org/10.1016/S1773-2247(05)50086-8)

632 [39] N.A. Peppas, J. Wu, E.D. von Meerwall, Macromol. (1994)
633 <https://doi.org/10.1021/ma00098a017>

634 [40] V. Michailova, S. Titeva, R. Kotsilkova, E. Krusteva, E. Minkov, Int J Pharma.
635 (2000) [https://doi.org/10.1016/S0378-5173\(00\)00536-6](https://doi.org/10.1016/S0378-5173(00)00536-6)

636

Supplementary Files

This is a list of supplementary files associated with this preprint. Click to download.

- [supplementarymaterialFINAL.pdf](#)